

Review

Phosphatic Biomineralization in Scyphozoa (Cnidaria): A Review

Olev Vinn 

Institute of Ecology and Earth Sciences, University of Tartu, Ravila 14A, 50411 Tartu, Estonia; olev.vinn@ut.ee

Abstract: Phosphatic biomineralization is unknown in modern species of Scyphozoa (Cnidaria). However, some extinct groups of Scyphozoa, such as conulariids and *Sphenothallus*, were capable of secreting phosphatic exoskeletons. Both conulariids and *Sphenothallus* used apatite to improve the mechanical properties of their skeletons, which offered better protection than the non-biomineralized periderms. The skeletons of conulariids and *Sphenothallus* have a lamellar microstructure. The shell lamellae of conulariids are often pierced by tiny pores. Several apatitic mineral structures have been described in conulariids and *Sphenothallus*, including plywood-like structures. Different lattice parameters of the apatite indicate that the biomineralization mechanisms of the phosphatic cnidarians *Sphenothallus* and conulariids differed from each other.

Keywords: apatite; microstructure; ultrastructure; biomineralization; fossilization; Cnidaria



Citation: Vinn, O. Phosphatic Biomineralization in Scyphozoa (Cnidaria): A Review. *Minerals* **2022**, *12*, 1316. <https://doi.org/10.3390/min12101316>

Academic Editors:
Yannicke Dauphin, Fabio Nudelman
and Jean-Pierre Cuif

Received: 23 September 2022

Accepted: 17 October 2022

Published: 18 October 2022

Publisher's Note: MDPI stays neutral with regard to jurisdictional claims in published maps and institutional affiliations.



Copyright: © 2022 by the author. Licensee MDPI, Basel, Switzerland. This article is an open access article distributed under the terms and conditions of the Creative Commons Attribution (CC BY) license (<https://creativecommons.org/licenses/by/4.0/>).

1. Introduction

Subphylum Medusozoa (Cnidaria) comprises the classes Cubozoa, Hydrozoa, Scyphozoa, and Staurozoa, with Cubozoa (box jellies) and Staurozoa previously classified as orders within Scyphozoa. The modern members of Scyphozoa do not possess biomineralized periderms, but the situation was different from the Ediacaran to Triassic [1–3].

Conulariids are an extinct (Ediacaran–Triassic) group of marine invertebrates now generally accepted as scyphozoan cnidarians [1,4–13]. They have a finely lamellar periderm that is composed of apatite [1,2,12,14]. Many previous authors have suggested that the conulariid periderm is an ectodermal derivative that grew by accretion of whole lamellae to its inner surface (centripetal accretion) and/or by extension of the periderm along its apertural margin [15].

Sphenothallus is an extinct genus of marine phosphatic tubicolous fossils known from the early Cambrian [16,17] to the Carboniferous [18] and it has an almost global distribution. *Sphenothallus* has been affiliated variously with conulariids [19] and hydroids due to their slightly conical shells. In the “Treatise on Invertebrate Paleontology”, [20] it was placed among the conulariids. Some authors have affiliated it with annelid worms [21], whereas others have allied with cnidarians [14,22]. The latter opinion has recently been supported by most of the authors and there is general agreement that *Sphenothallus* is a scyphozoan [9,16,17,23].

Torelrella is an extinct genus of slightly conical, phosphatic tubicolous marine organisms of unknown biological affinity. They have been allied either with annelids [24] or cnidarians [25]. Based on the apatitic composition of the periderm and the microlamellar structure, one could compare *Torelrella* with *Sphenothallus*. It is likely that *Torelrella* was a *Sphenothallus*-like scyphozoan.

The aim of the present paper is to review known mineral microstructures and mineral compositions of fossil scyphozoans, and to discuss their biomineralization.

2. Materials and Methods

All below illustrated sections of phosphatic cnidarian skeletons are natural surfaces photographed using scanning electron microscopy (SEM). Some samples were gold sput-

tered prior to SEM study. The specimens of *Torellella* from the Upper Cambrian of Estonia were coated with gold and photographed with a Jeol SEM at the University of Technology in Tallinn. The specimens of *Sphenothallus* from the Ordovician of Estonia were photographed uncoated with a variable pressure Zeiss EVO MA15 SEM at the Department of Geology, University of Tartu. The photos were taken using a backscattered electron detector (BSE) in a low vacuum regime. The beam voltage was 20 kV. The specimens of *Sphenothallus* and *Holoconularia* from the Carboniferous of Russia were coated with gold and palladium and photographed with the scanning electronic microscopes SEM TESCAN VEGA II and III at the Palaeontological Institute of the Russian Academy of Sciences in Moscow, where images of the shell structure were made using two detectors (SE and BSE). The illustrated specimens are deposited in the collections of the Natural History Museum, University of Tartu and Palaeontological Institute of the Russian Academy of Sciences. A crystal unit cell is characterized by its dimensions (length), which are of form *a*, *b* and *c* with three edges. These edges may or may not be mutually perpendicular.

3. Fossil Scyphozoa with Mineralized Test and Phosphatic Composition

Only some fossil scyphozoans biomineralized. Phosphatic skeletons occur in all genera of conulariids and in *Sphenothallus* and *Torellella* (Table 1). The conulariid genera are divided into two suborders: Circoconulariina Bischoff and Conulariina Miller and Gurley. The systematic position of *Sphenothallus* and *Torellella* within Scyphozoa remains unresolved (Table 1). The data on microstructure and/or mineralogy are only known for *Archaeoconularia*, *Baccaconularia*, *Conularia*, *Conularina*, *Climacoconus*, *Ctenoconularia*, *Eoconularia*, *Exoconularia*, *Holoconularia*, *Metaconularia*, *Paraconularia* and *Pseudoconularia* [2,4,14,25–27].

Table 1. The classification of fossil Scyphozoa. Genera with phosphatic skeletons indicated with bold font.

Classification	Genera	Stratigraphic Ranges
Suborder Circoconulariina Bischoff	<i>Australoconularia</i> Bischoff	Upper Silurian (Ludlovian)
	<i>Circonularia</i> Bischoff	Lower Silurian (Llandoveryan)
	<i>Garraconularia</i> Bischoff	Lower Silurian (Llandovery)- Lower Devonian (Lockhovian)
	<i>Sinusconularia</i> Hergarten	Lower Devonian (Lower Siegenian)
Suborder Conulariina Miller and Gurley	<i>Anaconularia</i> Sinclair	Middle Ordovician (Dapingian)- Upper Ordovician (Katian)
	<i>Archaeoconularia</i> Bouček	Lower Ordovician (Tremadoc)- Middle Silurian (Wenlock)
	<i>Baccaconularia</i> Hughes, Gunderson, and Weedon	Cambrian (Furongian)
	<i>Cheliconularia</i> Waterhouse	?Upper Carboniferous
	<i>Climacoconus</i> Sinclair	Early?/Middle Ordovician- Lower Devonian (?Middle Devonian)
	<i>Conularia</i> Miller in Sowerby	Middle Ordovician- Upper Mississippian
	<i>Conulariella</i> Bouček	Lower Ordovician (Floian)- Middle Ordovician (Darriwilian)
	<i>Conularina</i> Sinclair	Upper Ordovician
	<i>Ctenoconularia</i> Sinclair	Upper Ordovician-Lower Silurian
	<i>Eoconularia</i> Sinclair	Lower Ordovician-Lower Silurian
	<i>Galliconularia</i> Van Iten and Lefebvre	Lower Ordovician (Tremadocian-Floian)
	<i>Glyptoconularia</i> Sinclair	Upper Ordovician (Katian)
	<i>Metaconularia</i> Foerste	Middle Ordovician (Darriwilian)- Upper Silurian (Pridolian)
	<i>Microconularia</i> Percival	Upper Ordovician (late Eastonian-early Bolindian)
<i>Notoconularia</i> Thomas	Upper Carboniferous-Permian	
<i>Paraconularia</i> Sinclair	Terminal Ediacaran-Terminal Triassic	
<i>Pseudoconularia</i> Bouček	Lower Ordovician-Upper Silurian	

Table 1. Cont.

Classification	Genera	Stratigraphic Ranges
Order Incertae sedis	<i>Reticulaconularia</i> Babcock and Feldmann	Lower Devonian–Middle Devonian
	<i>Teresconularia</i> Leme and others	Lower Ordovician (Tremadocian)
	<i>Byronia</i> Matthew	Lower Cambrian–Permian
	<i>Cambrorhytium</i> Conway Morris and Robison	Lower Cambrian—Middle Cambrian
	<i>Cambrovitus</i> Mao, Zhao, Yu, and Qian	Lower Middle Cambrian (Series 2)
	<i>Paiutitubulites</i> Tynan	Lower Cambrian (Terreneuvian): Lower Cambrian (Series 2)–Upper Carboniferous
	<i>Sphenothallus</i> Hall	Lower Cambrian–upper Cambrian
	<i>Torellella</i> Holm <i>Tubulella</i> Howell	Middle Cambrian

4. Skeletal Microstructures and Mineral Composition of Conulariids

The conulariid periderm is made up of phosphatic lamellae. Typical conulariid resembles an ice-cream cone with fourfold symmetry and usually four prominently-grooved corners (Figure 1).

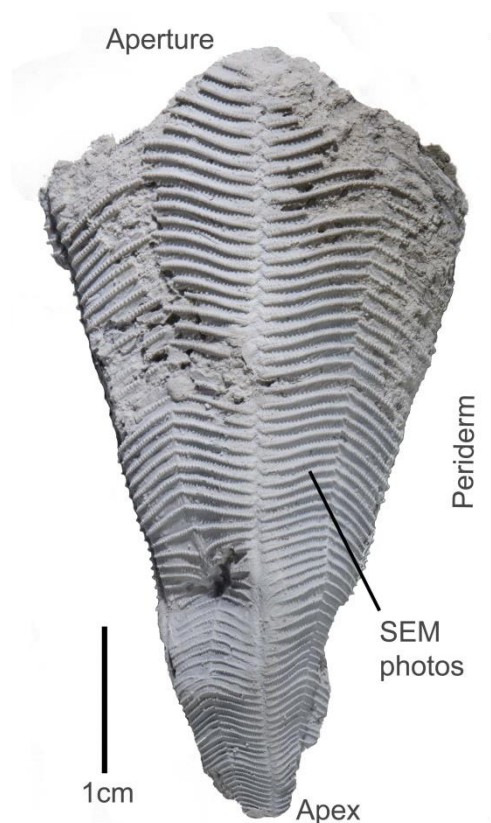


Figure 1. Periderm of a conulariid (*Holoconularia*) showing location of SEM images. The conulariid anatomy is based on Ford et al. [14].

4.1. Skeletal Structures

4.1.1. Microlamellar Fabric

The microlamellar fabric (Figure 2) is composed of extremely thin (approximately 0.5–3 μm) microlamellae that are alternately organic poor and organic rich [4,15]. The boundaries of microlamellae are variably distinct. Organic-rich microlamellae are interconnected by slender strands of organic matter that are embedded in calcium phosphate [4,15]. Microlamellae may be organized in thicker (approximately 5–75 μm) layers, or macrolamellae, that have variable organic matter content [4,14]. The thickness of macrolamellae

can vary within a single specimen. The surfaces of lamellae are smooth or pierced with microscopic pores. The microlamellar fabric has been reported in *Archaeoconularia*, *Baccaconularia*, *Conularia*, *Conularina*, *Climacoconus*, *Holoconularia*, *Metaconularia*, *Paraconularia*, and *Pseudoconularia* [2,4,15].

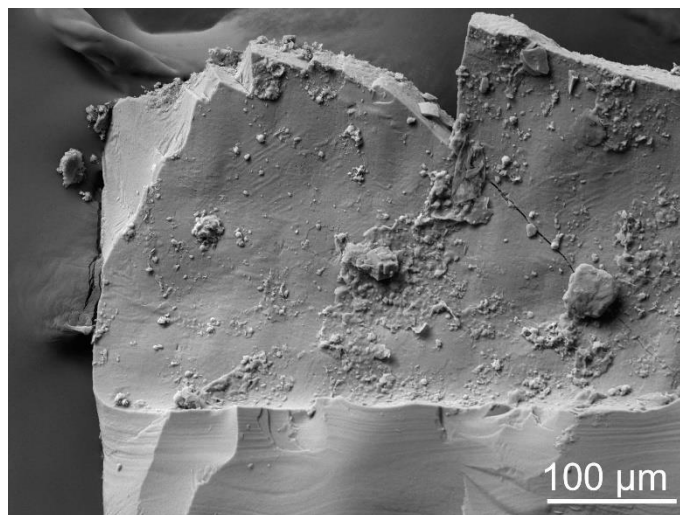


Figure 2. Microlamellar fabric in *Holoconularia* from the Carboniferous of Russia.

4.1.2. Micropores

In many conulariids, shell lamellae exhibit locally abundant, microscopic circular pores [26–28]. Owing probably to variation in the inclination of the micropores to the microlamellae, the rim of the micropores is usually circular to subcircular, but in some cases it may also be elliptical [29]. Micropores with circular rims are probably oriented with the axis of the pore channel perpendicular to the surface of the microlamellae, whereas those with elliptical rims are probably inclined, and thus represent oblique sections (Figure 3). Both circular and elliptical rims may occur on the same surface, their arrangement is random and shapes are transitional; that is, there are no discrete rim types [29]. The diameters of the pores range from approximately 2 μm to approximately 12 μm . In some specimens, the pores are relatively sparse (i.e., about eight pores per 1 mm^2) whereas in most specimens, the pores are numerous, with up to about 100 pores in an area of only 0.1 mm^2 [28]. The pores have been reported from *Archaeoconularia*, *Baccaconularia*, *Conularia*, *Conularina*, *Climacoconus*, *Ctenoconularia*, *Eoconularia*, *Exoconularia*, *Holoconularia*, *Metaconularia*, *Paraconularia* and *Pseudoconularia* [26–28].

4.2. Skeletal Microstructures

Homogeneous Granular Structure

The structure of the exfoliation surfaces is uniformly granular (Figure 2), with individual granules ranging from 0.3 to 1.0 μm in diameter in *Holoconularia* from the Carboniferous of Russia [29]. The polished and etched and polished samples of *Paraconularia* and *Conularia* periderm also show a homogeneous structure [14]. The structure has been reported from *Archaeoconularia*, *Baccaconularia*, *Conularia*, *Conularina*, *Climacoconus*, *Holoconularia*, *Metaconularia*, *Paraconularia*, and *Pseudoconularia* [2,4,15].

4.3. Mineral Composition

Vinn and Kirismäe [14] reported a conulariid (*Conularia* sp.) from the Upper Ordovician oil shale of Estonia, which is composed of francolite with a carbonate ion concentration 8.1 wt%. The lattice parameters of *Conularia* sp. apatite from the Upper Ordovician are $a = 9.315(7)$ Å, $c = 6.888(3)$ Å.

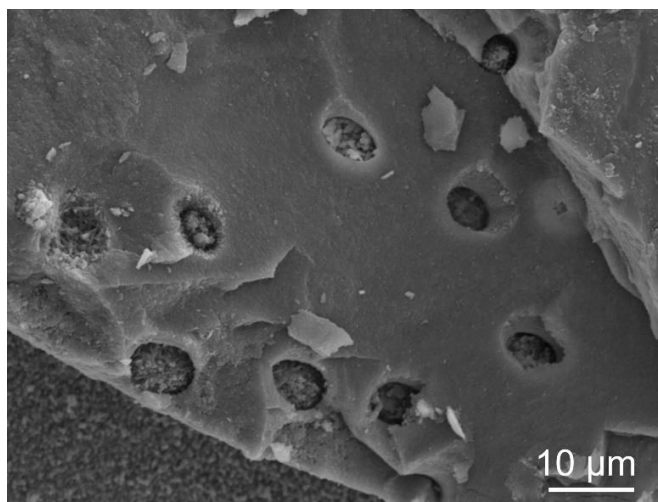


Figure 3. Micropores and homogeneous granular structure in *Holoconularia* from the Carboniferous of Russia.

5. Skeletal Microstructures and Mineral Composition of *Sphenothallus*

The periderm of *Sphenothallus* is made up of phosphatic lamellae and it has a tubular shape (Figure 4).

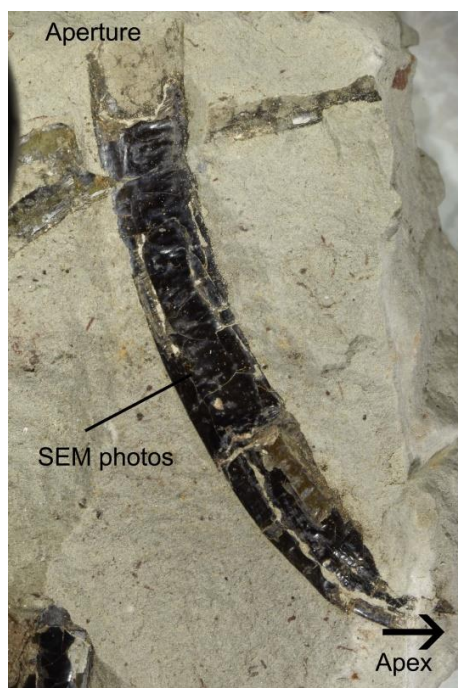


Figure 4. Periderm of *Sphenothallus* sp. from the Carboniferous of Russia. Location of SEM images indicated.

5.1. Skeletal Structures

5.1.1. Microlamellar Fabric

The structure is formed by a succession of thin apatitic lamellae (Figure 5) [14,30,31]. The development and thickness of the lamellae are variable within a single specimen. The lamellae are 3 to 170 μm thick [14,31]. The thickest lamellae occur in the external part of the tube wall at the lateral thickenings, whereas the thinnest lamellae are most common in the inner parts of the tube wall away from the lateral thickenings of the tube [31]. The

boundaries of the lamellae usually have variable sharpness, a common characteristic of both Ordovician and Carboniferous material [14,31]. Some boundaries constitute real gaps in the mineral structure, whereas others are artefacts caused by differences in crystal size and appear as parallel zones in the tube wall of *Sphenothallus*. The sharpness of the boundaries of individual lamella can change laterally within the tube [14,31].

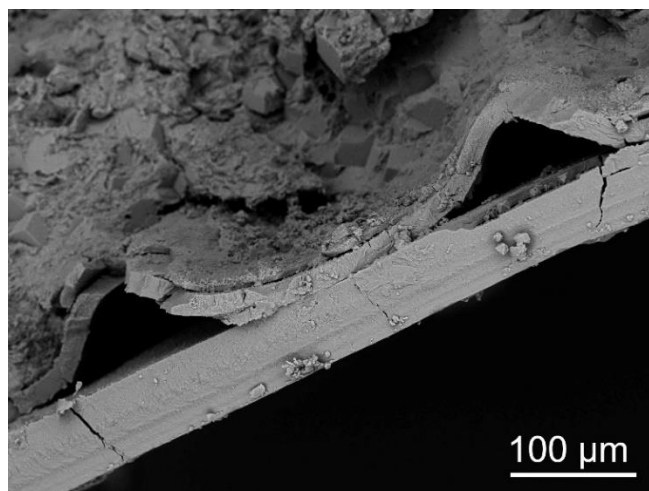


Figure 5. Microlamellar fabric and wrinkled lamella in *Sphenothallus* sp. from the Carboniferous of Russia.

5.1.2. Wrinkled Lamellae

There are laminae in *Sphenothallus* from the Carboniferous of Russia which have a wavy structure (Figure 5), and some lamellae are so wrinkled that they form hollow “ribs” within the tube wall, mostly in the lateral parts of the tube, where the wall is thickest [31].

5.1.3. Cylindrical Shafts

There are 2.0–2.5 μm wide cylindrical shafts (Figure 6) visible on the surface of an inner lamella of *Sphenothallus* from the Carboniferous of Russia [31]. These structures are preserved mostly in the form of shallow, slightly curved to straight grooves on the surfaces of the lamella, but some extend to the interior of the lamella in the form of cylindrical shafts. The lamellae with shafts have a smooth surface and are not composed of fibres. The entire surface of the lamellae is crowded with grooves and shafts [31].

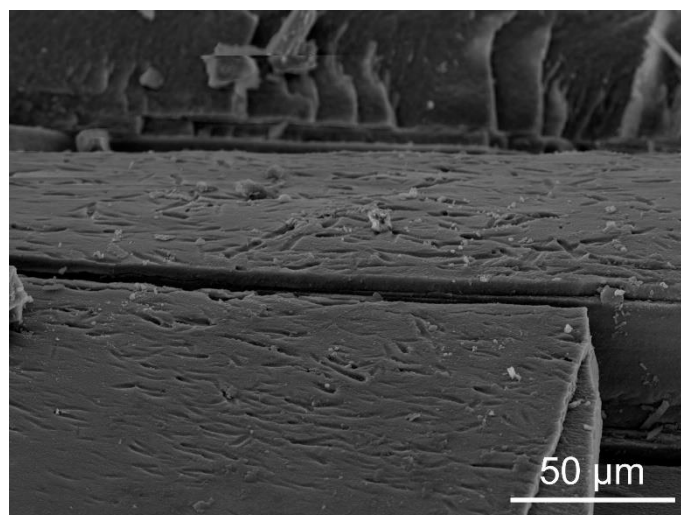


Figure 6. Cylindrical shafts in the lamella of *Sphenothallus* sp. from the Carboniferous of Russia.

5.2. Skeletal Microstructures

5.2.1. Homogeneous Granular Structure

The structure is composed of apatite in the form of subspherical crystallites measuring <500 nm in maximum diameter (Figure 7). The crystal size of apatite forming the homogeneous microstructure is variable and can be larger near the inter-lamellar boundaries [14].

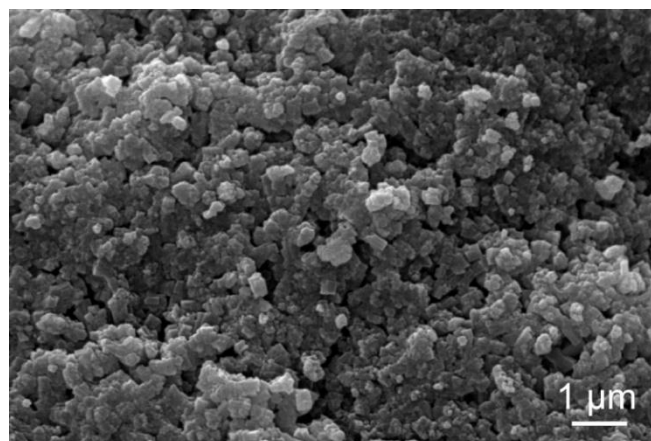


Figure 7. Homogeneous granular structure in *Sphenothallus* sp. from the Upper Ordovician of Estonia.

5.2.2. Plywood Structure

This structure consists of fibres (Figure 8) which are best observed in lateral parts of the tube wall [31]. The fibrous layers in the tube wall can be up to 70 μm thick. The fibres are at least tens of micrometres long and 1.5–2.0 μm thick. All fibres are parallel to the surface of the tube wall. The fibres within individual lamellae have the same, but in successive laminae they differ in orientation by irregularly varying angles. This structure occurs only in *Sphenothallus* from the Carboniferous of Russia [31].

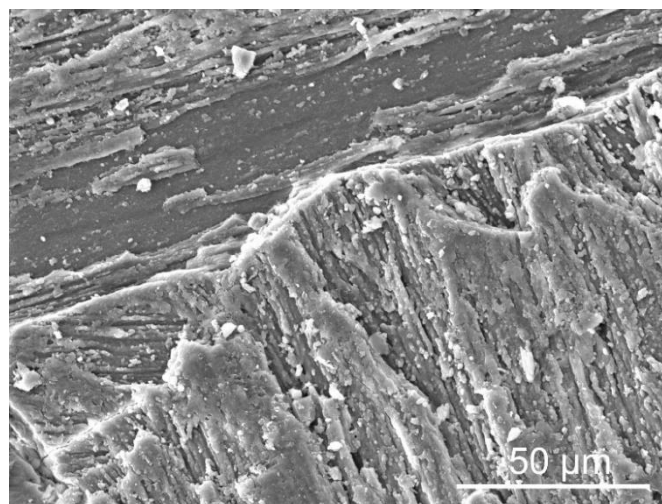


Figure 8. Plywood structure in *Sphenothallus* sp. from the Carboniferous of Russia.

5.3. Mineral Composition

The tubes of *Sphenothallus* aff. *longissimus* from the Ordovician of Estonia are composed of carbonate-substituted fluorapatite-francolite (Figure 9) [14]. The carbonate ion concentrations in the Ordovician *Sphenothallus* varies between 9.0–10.7 wt%. The lattice parameters of the apatite in the Ordovician *Sphenothallus* are [14]: Kohtla Nõmme specimen $a = 9.319(6) \text{ \AA}$, $c = 6.903(0) \text{ \AA}$; Kohtla specimen $a = 9.320(5) \text{ \AA}$, $c = 6.904(1) \text{ \AA}$; Kiviõli specimen $a = 9.321(7) \text{ \AA}$, $c = 6.904(1) \text{ \AA}$.

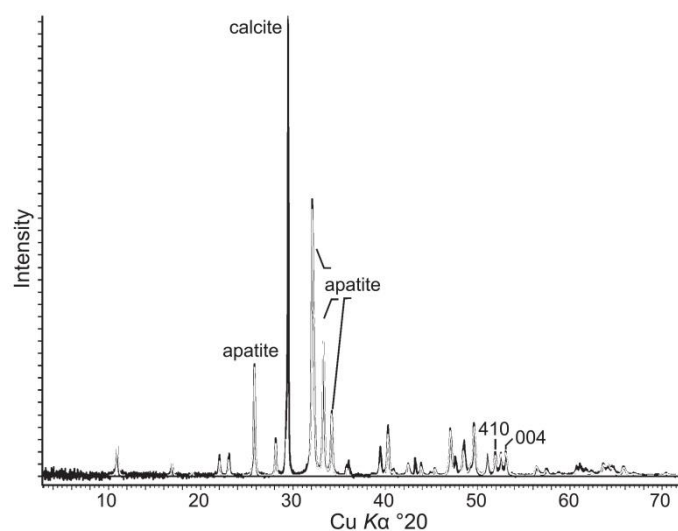


Figure 9. X-ray diffraction pattern of *Sphenothallus* sp. from the Upper Ordovician of Estonia [14].

An EDX analysis of a Carboniferous *Sphenothallus* by Vinn and Mironenko (2021) [31] detected no differences in elemental composition between smooth, fibrillar and globular layers of the *Sphenothallus* tube; they are all phosphatic.

6. Skeletal Microstructures and Mineral Composition of *Torellella*

The periderm of *Torellella* is made up of phosphatic lamellae and it has a tubular shape (Figure 10).

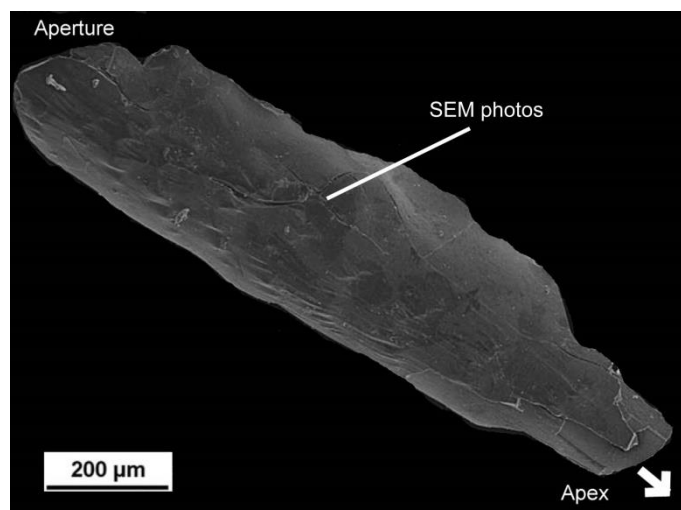


Figure 10. Periderm of *Torellella* from the upper Cambrian of Estonia. Location of SEM images indicated.

6.1. Skeletal Structures

Microlamellar Fabric

The tubes of *Torellella sulcata* from the upper Cambrian of Estonia exhibit lamellae of variable thickness (Figure 11). The original tube structure seems to be microlamellar with growth laminae about 1 μm thick. The surfaces of the lamellae are smooth without any perforations and have either homogeneous granular or fibrous ultrastructure [25].

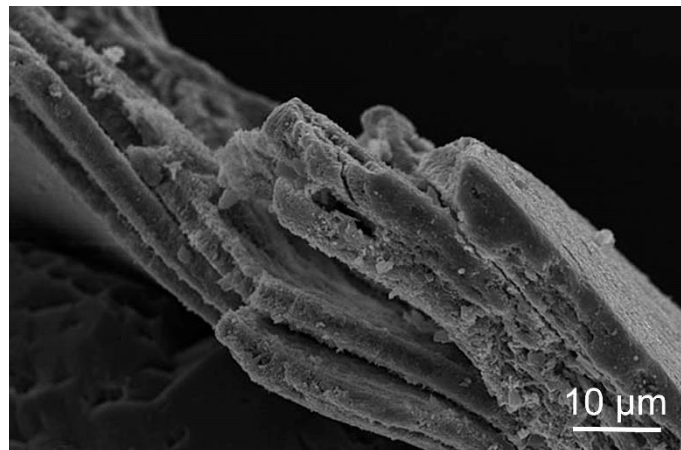


Figure 11. Microlamellar fabric in *Torellella sulcata* from the upper Cambrian of Estonia.

6.2. Skeletal Microstructures

6.2.1. Homogeneous Globular Structure

This structure (Figure 12) consists of somewhat rounded phosphatic crystallites. The crystallites are 0.20 to 0.25 μm in diameter. Lamellae which are composed of homogeneous globular structure are often thicker than 10 μm [25].

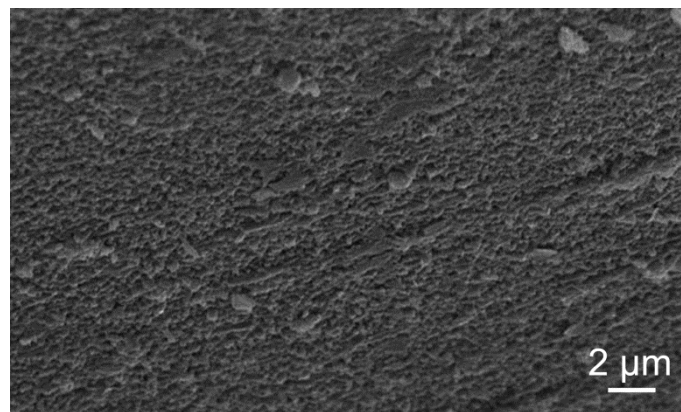


Figure 12. Homogeneous globular structure in *Torellella sulcata* from the upper Cambrian of Estonia.

6.2.2. Fibrous Structure

This structure (Figure 13) consists of fibres that have same orientation within the growth lamellae and are parallel to the surface of the tube wall. The fibres are 0.2–0.3 μm thick and about 4–6 μm long [25]. In *T. gracilenta* from the lower Cambrian of Siberia, each lamella is composed of fibres; neighboring lamellae contain variously directed fibres [24].

6.3. Mineral Composition

The X-ray structural analysis performed by Esakova and Zhegallo [32] showed that tubes of *Torellella lentiformis* from the Lower Cambrian of the Siberian Platform and *T. gracilenta* from the lower Cambrian of Mongolia consist of francolite (i.e., carbonate rich fluorapatite).

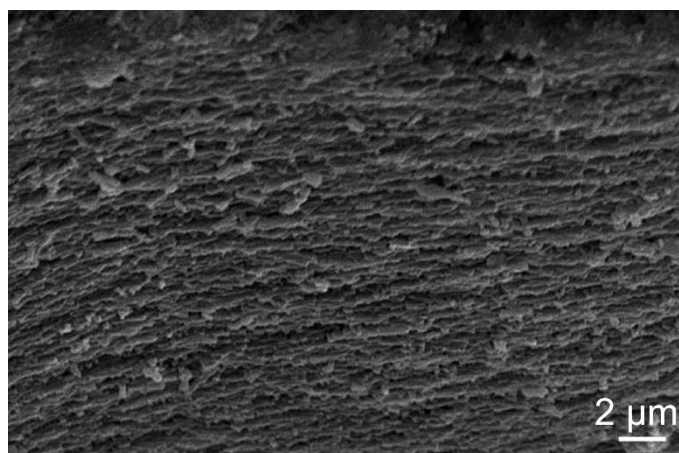


Figure 13. Fibrous structure in *Torelrella sulcata* from the upper Cambrian of Estonia.

7. Discussion

7.1. Biomineralization in Conulariids

The secretion of the conulariid periderm was likely cyclic. The conulariids secreted cyclically organic-rich and organic-poor mucus, which allowed the creation of periderm composed of alternating organic-rich and organic-poor apatitic lamellae [14]. The conulariid started to secrete its periderm beginning with the outermost lamella. It is not known whether the conulariids started to build their periderm with organic-rich lamellae or vice versa with organic-poor, mostly mineral lamellae. However, one could hypothesize that organic-rich lamellae may have served as a scaffold for the biomineralization of organic-poor mineral lamellae. Organic matrices in skeletons in general serve as templates for biomineralization [33–35], but they also add tensile and elastic strength to the mineral component [15], thus forming a strong biocomposite material. There is a striking similarity between composite materials and the conulariid periderm [15]. Composite materials have one component with good mechanical strength, such as apatite in conulariids, and another with good elastic properties, such as organic-rich lamellae in conulariids [15]. Such composite materials perform much better under all kinds of stresses than shells made of purely rigid or elastic materials [35,36]. The pores in conulariid lamellae were likely part of the original shell structure [29]. They may have also served the function of enhancing the mechanical properties of the mineral lamellae if they were filled with elastic organic material. In addition, or alternatively, they may have supported the biomineralization of mineral lamellae if they contained organic matrix. The conulariids exhibit a single, simple homogeneous granular ultrastructure. The lack of diverse microstructures in conulariids contrasts with the otherwise complex architecture of their periderm. It is possible that the conulariids' biomineralization mechanism was unable to control the orientation of the crystallographic axis of individual crystals.

7.2. Biomineralization in *Sphenothallus*

Some macrolamellae form hollow ribs in Carboniferous *Sphenothallus* from Russia. It is possible that lamellae with a higher organic content became wrinkled, owing to contraction after the decay of the organic material [31]. This may indicate that the content of organic matter varied between different macrolamellae. The wrinkled macrolamellae cannot be directly compared to organic-rich microlamellae in conulariids due to their large differences in thickness. However, the biomineralization system of *Sphenothallus* was clearly capable of secreting lamellae with different compositions.

There are cylindrical shafts in the lamella of *Sphenothallus* from the Carboniferous of Russia. The orientation of cylindrical shafts (sub-parallel to the surface of lamella) and their morphology indicates that they presumably were not part of the original shell structure of *Sphenothallus*, but are actually borings [31]. These borings are different from the pores found

in conulariids [28] and their size corresponds to microbioerosion. It is likely that some lamellae of *Sphenothallus* periderm were bored by some chemical means by microorganisms feeding on the organic compounds of the lamella [31].

It is generally agreed that the original composition of *Sphenothallus* tubes was organo-phosphatic [9,22,30]. However, it is not clear which microstructures were originally apatitic and which might be phosphatized organic tissues. The homogenous granular microstructure of *Sphenothallus* is similar to that of conulariids' periderm microstructure and is either an original peridermal structure or the result of diagenetic alternation of the original apatitic structure. The plywood structure is more difficult to interpret, as there is no analogy among phosphatic invertebrate skeletal microstructures [37]. There are two possibilities: the plywood structure could be either phosphatized organic tissue, or it is an original biomineral apatitic structure. In the latter case, the biomineralization of *Sphenothallus* was extremely advanced and different from that of conulariids, being comparable only to that of vertebrates.

7.3. Biomineralization in *Torelrella*

Vinn [25] interpreted the fibrous structure of *Torelrella* as an original biomineral ultrastructure of the tube. The plywood structure in *Sphenothallus* is similar to the fibrous lamellae in *Torelrella* and may also have a similar origin. The biomineralization of *Torelrella* seems to resemble more that of *Sphenothallus* than of conulariids. This is not surprising, considering the fact that *Torelrella* is morphologically closer to *Sphenothallus* than to conulariids.

7.4. Biomineralization in *Scyphozoa*

The scyphozoans possess just two types of skeletal microstructures, far fewer than the 15 types of calcareous microstructures present in anthozoans. This may indicate that calcareous biomineralization was better suited for the physiology of cnidarians. Medusozoans possess the highest number of known phosphatic microstructures in Cnidaria, though still fewer than the number of known phosphatic structures in brachiopods [37].

The skeletal microstructures, and likely also the processes of skeletogenesis, are similar in conulariids, *Sphenothallus* and *Torelrella*, but they are somewhat different from those of other phosphatic invertebrates, such as brachiopods. The mineral composition of the scyphozoan periderm is also similar in conulariids, *Sphenothallus* and *Torelrella*, with all three taxa being composed of francolite (i.e., carbonate rich fluorapatite) [14]. Nevertheless, there are some differences between the lattice parameters of *Conularia* and *Sphenothallus* (Figure 14), though their apatites are somewhat similar to that of fossil *Lingula* and sedimentary apatites. The latter similarity is presumably due to the fossilization process.

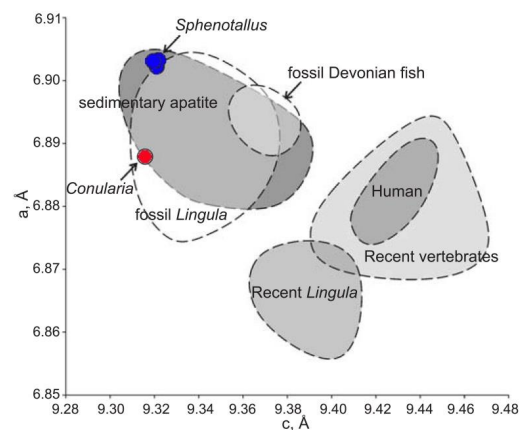


Figure 14. Lattice parameters of *Sphenothallus* apatite compared with *Conularia* and other biological and sedimentary apatites [14]. The length of unit cell edges: a and c. Data about other organisms and sedimentary apatites from Nemliher [38].

8. Conclusions

The skeletal microstructures, and likely also the processes of skeletogenesis, are similar in all fossil scyphozoans. All fossil scyphozoans (i.e., conulariids, *Sphenothallus* and *Torelrella*) have a microlamellar periderm composed of francolite. The plywood structure in *Sphenothallus* and the fibrous structure in *Torelrella* could be either phosphatized organic tissues or original biomineral apatitic structures. In the latter case, the biomineralization of *Sphenothallus* and *Torelrella* was extremely advanced compared with those of other phosphatic invertebrates. The lack of diverse ultrastructures in conulariids contrasts with the otherwise complex architecture of their periderm, indicating that the biomineralization mechanism of conulariids was incapable of controlling the crystallographic orientation of individual crystallites.

Funding: Financial support to O.V. was provided by a research grant from the Institute of Ecology and Earth Sciences, University of Tartu.

Data Availability Statement: Not applicable.

Acknowledgments: I am grateful to K. Kirsimäe, Department of Geology, University of Tartu and A.A. Mironenko, Geological Institute of Russian Academy of Sciences, for taking the SEM images. I am grateful to H. Van Iten and two anonymous reviewers for their constructive comments on the manuscript.

Conflicts of Interest: The author declares no conflict of interest. The funders had no role in the design of the study; in the collection, analyses, or interpretation of data; in the writing of the manuscript; or in the decision to publish the results.

References

1. Van Iten, H. Anatomy and phylogenetic significance of the corners and midlines of the conulariid test. *Palaeontology* **1992**, *35*, 335–358.
2. Van Iten, H. Microstructure and growth of the conulariid test: Implications for conulariid affinities. *Palaeontology* **1992**, *35*, 359–372.
3. Van Iten, H.; Leme, J.M.; Pacheco, M.L.A.F.; Simões, M.G.; Fairchild, T.R.; Rodrigues, F.; Galante, D.; Boggiani, G.C.; Marques, A.C. Origin and early diversification of phylum Cnidaria: Key macrofossils from the Ediacaran System of North America. In *The Cnidaria, Past, Present and Future*; Goffredo, S., Dubinsky, Z., Eds.; Springer: Berlin/Heidelberg, Germany, 2016; pp. 31–40.
4. Jerre, F. Anatomy and phylogenetic significance of *Eoconularia loculata*, a conulariid from the Silurian of Gotland. *Lethaia* **1994**, *27*, 97–109. [[CrossRef](#)]
5. Hughes, N.C.; Gundersen, G.O.; Weedon, M.J. Late Cambrian conulariids from Wisconsin and Minnesota. *J. Paleontol.* **2000**, *74*, 828–838. [[CrossRef](#)]
6. Van Iten, H.; Leme, J.M.; Simões, M.G.; Marques, A.C.; Collins, A.G. Reassessment of the phylogenetic position of conulariids (?Ediacaran–Triassic) in the subphylum Medusozoa (phylum Cnidaria). *J. Syst. Palaeontol.* **2006**, *4*, 109–118. [[CrossRef](#)]
7. John, D.L.; Hughes, N.C.; Galaviz, M.I.; Gundersen, G.O.; Meyer, R. Unusually preserved *Metaconularia manni* (Roy, 1935) from the Silurian of Iowa, and the systematics of the genus. *J. Paleontol.* **2010**, *84*, 1–31. [[CrossRef](#)]
8. Robson, S.P.; Young, G.A. Late Ordovician conulariids from Manitoba, Canada. *J. Paleontol.* **2013**, *87*, 775–785. [[CrossRef](#)]
9. Van Iten, H.; Muir, L.A.; Botting, J.P.; Zhang, Y.D.; Lin, J.P. Conulariids and *Sphenothallus* (Cnidaria, Medusozoa) from the Tonggao Formation (Lower Ordovician, China). *Bull. Geosci.* **2013**, *88*, 713–722. [[CrossRef](#)]
10. Van Iten, H.; Burkey, M.H.; Leme, J.M.; Marques, A.C. Cladistics and mass extinctions: The example of conulariids (Scyphozoa, Cnidaria) and the End Ordovician Extinction Event. *GFF* **2014**, *136*, 275–280. [[CrossRef](#)]
11. Van Iten, H.; Marques, A.C.; Leme, J.M.; Pacheco, M.L.A.F.; Simões, M.G. Origin and early diversification of the phylum Cnidaria Verrill: Major developments in the analysis of the taxon’s Proterozoic–Cambrian history. *Palaeontology* **2014**, *57*, 677–690. [[CrossRef](#)]
12. Van Iten, H. Anatomy, pattern of occurrence, and nature of the conulariid schott. *Palaeontology* **1991**, *34*, 939–954.
13. Leme, J.M.; Van Iten, H.; Simões, M.G. A New Conulariid (Cnidaria, Scyphozoa) From the Terminal Ediacaran of Brazil. *Front. Earth Sci.* **2022**, *10*, 777746. [[CrossRef](#)]
14. Vinn, O.; Kirsimäe, K. Alleged cnidarian *Sphenothallus* in the Late Ordovician of Baltica, its mineral composition and microstructure. *Acta Palaeontol. Pol.* **2015**, *60*, 1001–1008. [[CrossRef](#)]
15. Ford, R.C.; Van Iten, H.; Clark, G.R., II. Microstructure and composition of the periderm of conulariids. *J. Paleontol.* **2016**, *90*, 389–399. [[CrossRef](#)]
16. Zhu, M.; Iten, H.; Cox, R.; Zhao, Y.; Erdtmann, B. Occurrence of *Byronia* Matthew and *Sphenothallus* Hall in the lower Cambrian of China. *Palaeontol. Z.* **2000**, *74*, 227–238. [[CrossRef](#)]

17. Li, G.-X.; Zhu, M.-Y.; Van Iten, H.; Li, C.-W. Occurrence of the earliest known *Sphenothallus* Hall in the lower Cambrian of Southern Shaanxi Province, China. *Geobios* **2004**, *37*, 229–237. [[CrossRef](#)]
18. Neal, M.L.; Hannibal, J.T. Paleoecologic and taxonomic implications of *Sphenothallus* and *Sphenothallus*-like specimens from Ohio and areas adjacent to Ohio. *J. Paleontol.* **2000**, *74*, 369–380. [[CrossRef](#)]
19. Ruedemann, R.H. Note on the discovery of a sessile Conularia. *Am. Geol.* **1896**, *17*, 158–165.
20. Moore, R.C.; Harrington, H.J. Conulata. In *Treatise on Invertebrate Paleontology, Pt. F, Coelenterata*; Moore, R.C., Ed.; Geological Society of America and University of Kansas Press: Lawrence, NY, USA, 1956; pp. F54–F66.
21. Mason, C.; Yochelson, E.L. Some tubular fossils (*Sphenothallus*: “Vermes”) from the middle and late Paleozoic of the United States. *J. Paleontol.* **1985**, *59*, 85–95.
22. Van Iten, H.; Fitzke, J.A.; Cox, R.S. Problematical fossil cnidarians from the Upper Ordovician of the north-central USA. *Palaeontology* **1996**, *39*, 1037–1064.
23. Peng, J.; Babcock, L.E.; Zhao, Y.; Wang, P.; Yang, R. Cambrian *Sphenothallus* from Guizhou Province, China: Early sessile predators. *Palaeogeogr. Palaeoclimatol. Palaeoecol.* **2005**, *220*, 119–127. [[CrossRef](#)]
24. Demidenko, Y.E. Morphology and Systematic Position of the Cambrian Zooproblematic *Torellella gracilentia* Esakova, 1996 (Order Hyolithelminthida Fisher, 1962). *Paleontol. J.* **2019**, *53*, 676–688. [[CrossRef](#)]
25. Vinn, O. Possible cnidarian affinities of *Torellella* (Hyolithelminthes, Upper Cambrian, Estonia). *Paläont. Z.* **2006**, *80*, 384–389. [[CrossRef](#)]
26. Bischoff, G.C.O. Internal structures of conulariid tests and their functional significance, with special reference to Circoconulariina n. suborder (Cnidaria, Scyphozoa). *Senck. Lethaia* **1978**, *59*, 275–327.
27. Van Iten, H.; Leme, J.M.; Rodrigues, S.C.; Simões, M.G. Reinterpretation of a conulariid-like fossil from the Vendian of Russia. *Palaeontology* **2005**, *48*, 619–622. [[CrossRef](#)]
28. Van Iten, H.; Vhylasová, Z.; Zhu, M.Y.; Qian, Y. Widespread occurrence of microscopic pores in conulariids. *J. Paleontol.* **2005**, *79*, 400–407. [[CrossRef](#)]
29. Van Iten, H.; Mironenko, A.A.; Vinn, O. A new conulariid from the Upper Mississippian (early Serpukhovian) of Central Russia (Moscow Basin): Systematics, microstructure, and growth abnormalities. *PalZ* **2022**, *97*, 1–12. [[CrossRef](#)]
30. Muscente, A.D.; Xiao, S. New occurrences of *Sphenothallus* in the lower Cambrian of South China: Implications for its affinities and taphonomic demineralization of small shelly fossils. *Palaeogeogr. Palaeoclimatol. Palaeoecol.* **2015**, *437*, 141–164. [[CrossRef](#)]
31. Vinn, O.; Mironenko, A.A. Discovery of plywood structure in *Sphenothallus* from Gurovo Formation (Mississippian), central Russia. *Ann. Soc. Geol. Pol.* **2021**, *91*, 67–74.
32. Esakova, N.V.; Zhegallo, E.A. Biostratigrafiya i fauna nizhnego kembriya Mongolii (Biostratigraphy and Fauna of the Lower Cambrian of Mongolia). *Tr. Sovm. Ross.-Mongol. Paleontol. Eksp.* **1996**, *46*, 1–216.
33. Addadi, L.; Weiner, S. Control and design principles in biological mineralization. *Angew. Chem. Int. Ed.* **1992**, *31*, 153–169. [[CrossRef](#)]
34. Cuif, J.P.; Dauphin, Y.; Sorauf, J.P. *Biominerals and Fossils through Time*; Cambridge University Press: Cambridge, UK, 2011; p. 490.
35. Mann, S. *Biomineralization: Principles and Concepts in Bioinorganic Materials Chemistry*; Oxford University Press: Oxford, UK, 2001; p. 198.
36. Jackson, A.P.; Vincent, J.F.V.; Turner, R.M. The mechanical design of nacre. *Proc. R. Soc. Lond. B* **1988**, *234*, 415–440. [[CrossRef](#)]
37. Carter, J.G.; Bandel, K.; de Burenil, V.; Carlson, S.J.; Castanet, J.; Crenshaw, M.A.; Dalingwater, J.E.; Francillion-Vieillot, H.; Geradie, J.; Meunier, F.J.; et al. Glossary of skeletal biomineralization. In *Skeletal Biomineralization: Patterns, Processes and Evolutionary Trends*; Carter, J.G., Ed.; Wiley: Hoboken, NJ, USA, 1990; pp. 609–671.
38. Nemliher, J. Mineralogy of Phanerozoic Skeletal and Sedimentary Apatites: An XRD Study. Ph.D. Thesis, Tartu University, Tartu, Estonia, 1999; p. 134.